

RESEARCH ARTICLE | JUNE 13 2022

Fully resonant magneto-elastic spin-wave excitation by surface acoustic waves under conservation of energy and linear momentum ^{EP}

Moritz Geilen ; Alexandra Nicoloiu; Daniele Narducci; ... et. al



Appl. Phys. Lett. 120, 242404 (2022)

<https://doi.org/10.1063/5.0088924>



CrossMark

Articles You May Be Interested In

Interference of co-propagating Rayleigh and Sezawa waves observed with micro-focused Brillouin light scattering spectroscopy

Appl. Phys. Lett. (November 2020)

Hybrid magnonic-oscillator system

Journal of Applied Physics (November 2022)

Dynamic response and reinforcement mechanism of composites embedded with tetra-needlelike ZnO nanowhiskers

Appl. Phys. Lett. (July 2007)



A total solution for low-temperature characterization

[Learn more >](#)



Fully resonant magneto-elastic spin-wave excitation by surface acoustic waves under conservation of energy and linear momentum

Cite as: Appl. Phys. Lett. **120**, 242404 (2022); doi: [10.1063/5.0088924](https://doi.org/10.1063/5.0088924)

Submitted: 21 February 2022 · Accepted: 31 May 2022 ·

Published Online: 13 June 2022







View Online



Export Citation



CrossMark

Moritz Geilen,^{1,a)}  Alexandra Nicoloiu,²  Daniele Narducci,^{3,4}  Morteza Mohseni,¹  Moritz Bechberger,¹  Milan Ender,¹ Florin Ciubotaru,³  Burkard Hillebrands,¹  Alexandru Müller,²  Christoph Adelman,³  and Philipp Pirro¹ 

AFFILIATIONS

¹Fachbereich Physik and Landesforschungszentrum OPTIMAS, Technische Universität Kaiserslautern, Kaiserslautern, Germany

²National Institute for Research and Development in Microtechnologies, Bucharest R-07719, Romania

³imec, Leuven B-3001, Belgium

⁴Departement Materiaalkunde, KU Leuven, 3001 Leuven, Belgium

^{a)} Author to whom correspondence should be addressed: mgeilen@physik.uni-kl.de

ABSTRACT

We report on the resonant excitation of spin waves in micro-structured magnetic thin films by short-wavelength surface acoustic waves (SAWs). The spin waves as well as the acoustic waves are studied by micro-focused Brillouin light scattering spectroscopy. At low magnetic bias fields, a resonant phonon–magnon conversion is possible, which results in the excitation of short-wavelength spin waves. Using micro-magnetic simulations, we verify that during this excitation both energy and linear momentum are conserved and fully transferred from the SAW to the spin wave. This conversion can already be detected after an interaction length of a few micrometers. Thus, our findings pave the way for miniaturized magneto-elastic spin-wave emitters for magnon computing.

© 2022 Author(s). All article content, except where otherwise noted, is licensed under a Creative Commons Attribution (CC BY) license (<http://creativecommons.org/licenses/by/4.0/>). <https://doi.org/10.1063/5.0088924>

The rapid increase in computing power in CMOS-based devices, which is described by Moore's law, has slowed down in recent years.¹ One reason for this is the drastic reduction in the component size combined with the Joule heating generated by the charge carriers. A promising complementary technology is magnonics,^{2–5} in which spin waves, whose quasi-particles are known as magnons, are used as information carriers. Unlike CMOS, magnonics proposes a wave-based logic in which the information can be encoded in both the amplitude and the phase of the spin waves.⁶ This also makes magnonic systems attractive for implementing neural networks.⁷ Over time, the functionality of various essential components such as transistors,⁸ diodes,^{9–11} majority gates,^{12–14} directional couplers,¹⁵ or half-adders¹⁶ was demonstrated. Due to the small wavelength and the GHz frequencies of spin waves, the necessary miniaturization of the magnonic components to the nanometer scale^{6,17} is possible. However, the efficient excitation of spin waves at these dimensions is challenging, since the commonly used technique of microwave current fed antennas suffers from Joule heating. This argues for

voltage-based excitation mechanisms, such as the use of multiferroic heterostructures.^{18–20} An alternative approach to voltage-controlled spin-wave excitation is to use magneto-elastic coupling between magnons and phonons²¹ since in piezoelectric materials, phonons can be excited in an energy-efficient way by means of electric fields. In this context, the coupling of spin waves with bulk acoustic waves (BAW)²² and surface acoustic waves (SAWs) is of great interest.^{23,24} It has been demonstrated that the excitation of spin waves by SAWs provides a damping channel for the latter. This has been exploited to realize non-reciprocal SAW propagation, e.g., using the Dzyaloshinskii–Moriya interaction.^{25,26} Most of these studies use SAW transmission spectroscopy,²⁷ while only a few take an optical approach to probe the phonon–magnon coupling.^{28–30} Similarly, most works concentrate on the SAW transmission and not on the properties of the excited spin waves. Thus, until now, the conservation of energy and momentum during the excitation process has not been shown, which is crucial for the implementation into magnonic circuits.

In this study, we investigate the excitation of spin waves by SAWs in micrometer-sized strips of cobalt–iron–boron ($\text{Co}_{40}\text{Fe}_{40}\text{B}_{20}$) thin films. We use micro-focused Brillouin light scattering spectroscopy (μBLS) to observe both SAWs and spin waves separately. This is possible due to the different rotation of the polarization of the light during the inelastic scattering process. We demonstrate that for a given SAW frequency f , resonances for the excitation of spin waves at the same frequency can be observed at two different magnetic bias fields. The excitation at higher fields can be identified as the ferromagnetic resonance (FMR). In this process, however, the wave vector could not be preserved in a phonon–magnon scattering process which hints at a defect mediated process or an excitation due to residual electromagnetic leakage. The second excitation at low bias fields corresponds to a wave vector-preserving excitation of spin waves. To illustrate the details of this resonant process, we use micromagnetic simulations which take into account the finite size of the magnetic elements as well as the (inhomogeneous) demagnetization fields inside them.

Brillouin light scattering³¹ is the inelastic scattering of photons with quasi-particles, like magnons or phonons, which makes it a favorable tool to probe the phonon–magnon interaction. During the scattering process, energy and momentum of the scattered quasi-particle is transferred to the photon. In order to obtain a sufficient spatial resolution, in this study, laser light ($\lambda_{\text{Laser}} = 532 \text{ nm}$) is focused onto the sample by a microscope objective with a magnification of $100\times$ and a numerical aperture of $\text{NA} = 0.75$. This results in spatial resolution down to 250 nm and a maximal detectable wave vector of $k_{\text{max}} = 16 \text{ rad}/\mu\text{m}$. The backscattered light is then collected by the same objective lens and subsequently the frequency shift of the scattered light is analyzed by a polarization-sensitive Tandem Fabry–Pèrot interferometer (TFPI). The investigated sample is shown in Fig. 1 and consists of an interdigital transducer (IDT), which has been fabricated on commercial GaN/Si wafer (produced by NTT-AT Japan). The undoped GaN layer ($1 \mu\text{m}$ thick) was grown on a high resistivity $\langle 111 \rangle$ oriented silicon wafer using a $0.3 \mu\text{m}$ thin AlN buffer layer. High-resolution x-ray diffraction spectra showed the presence of the Si substrate, the AlN layer, and the GaN layer. Multiple reflections of GaN show the presence of closed packing lattice planes along $\langle 0001 \rangle$

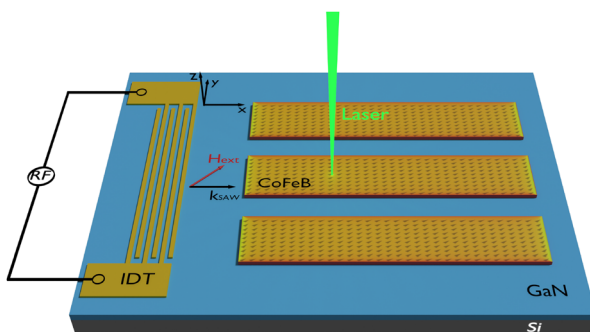


FIG. 1. Schematic illustration of the investigated structure (not to scale). SAWs are excited by interdigital transducers (IDTs) with 170 nm finger-to-finger spacing on a piezoelectric GaN layer. The CoFeB rectangles are $10 \mu\text{m}$ wide, $50 \mu\text{m}$ long, and 18 nm thick. The external bias field is applied with an angle of 45° to the SAW propagation direction which is equivalent to the long axis of the CoFeB rectangles.

direction. To excite SAWs an IDT with a finger-to-finger distance of 170 nm is used, which results in a resonantly excited SAW wavelength of $\lambda_{\text{SAW}} = 680 \text{ nm}$ ($k_{\text{SAW}} = 9.2 \text{ rad}/\mu\text{m}$). This results in the first harmonic resonance of the Rayleigh mode to be at a frequency of $f = 6.3 \text{ GHz}$. The IDT has been contacted by microwave probes with ground-signal-ground configuration and connected to an RF-generator. Further details about the phonon excitation and propagation in this particular structure are published in Ref. 32. It is known that due to the finite bandwidth of the IDT, the Rayleigh mode and the first Sezawa mode are excited simultaneously with the same frequency but different wavelengths. For these two modes, the displacement takes place exclusively in the x - z plane. Consequently, only the components S_{xx} and S_{xz} of the strain tensor have to be considered in the following. As shown in Fig. 1, rectangles of $\text{Co}_{40}\text{Fe}_{40}\text{B}_{20}$ are located in front of the IDT. These are $50 \mu\text{m}$ long, $10 \mu\text{m}$ wide, and have a thickness of 18 nm . Additionally, a single microstrip antenna (not shown in Fig. 1) with a width of $1 \mu\text{m}$ is structured over the magnetic rectangles which serves as a reference spin-wave source. The external magnetic field is applied in-plane and under an angle of $\varphi = 45^\circ$ to the wave vector of the SAWs. Under this condition, the magneto-elastic interaction is maximized²³ and a strong magneto-elastic spin-wave excitation by SAWs is expected.

First, the polarization of the inelastically scattered light is investigated in order to separate the signals originating from spin waves and SAWs. We use a $\lambda/2$ -plate in front of the polarization-sensitive TFPI to analyze the polarization of the inelastically scattered light. For this purpose, SAWs with the frequency $f = 6.3 \text{ GHz}$ were excited by means of the IDT. The measurement takes place on the CoFeB while a strong external magnetic field is applied which shifts the magnon band above the SAW frequency. Figure 2(a) shows the normalized BLS intensity as a function of polarization of the inelastically scattered light. For the SAWs (red), the polarization of the scattered light does not change with respect to the incident polarization. To generate a signal which is purely produced by scattering with spin waves, the reference microstrip antenna³³ and a microwave current with the same frequency and power is used. As expected, the polarization of the inelastically scattered light is rotated by $\pi/2$. Therefore, the intensity of magnons and phonons can be measured separately by selecting the appropriate polarizer setting.

In the following, the spin waves excited by SAWs are studied. For this purpose, a microwave with a frequency of $f = 6.3 \text{ GHz}$ and a power of $P = +5 \text{ dBm}$ (neglecting losses in connecting cables and connections) is applied to the IDT. A typical BLS spectrum is shown in Fig. 2(b). It can be seen that only spin waves around the applied RF-frequency are excited. The measurement of the magnons is carried out $2.8 \mu\text{m}$ away from the edge of the CoFeB rectangle facing the IDT. This measurement position guarantees that there are no additional influences due to the changed SAW amplitude, which can significantly be reduced on resonance if the SAW would propagate longer distances on the CoFeB. Only the portion of the light rotated by $\pi/2$ is analyzed. Figure 2(c) shows the extracted BLS intensity around $f = 6.3 \text{ GHz}$ for different external magnetic fields. Two maxima can be identified near $\mu_0 H_{\text{ext}} = 6 \text{ mT}$ and $\mu_0 H_{\text{ext}} = 33 \text{ mT}$, respectively. The maximum at the higher field values can be attributed to the excitation of the FMR.³⁴ Here, the energy conservation is fulfilled while the momentum conservation in a phonon–magnon conversion process would be broken. The second maximum is connected to a phase-matching excitation of

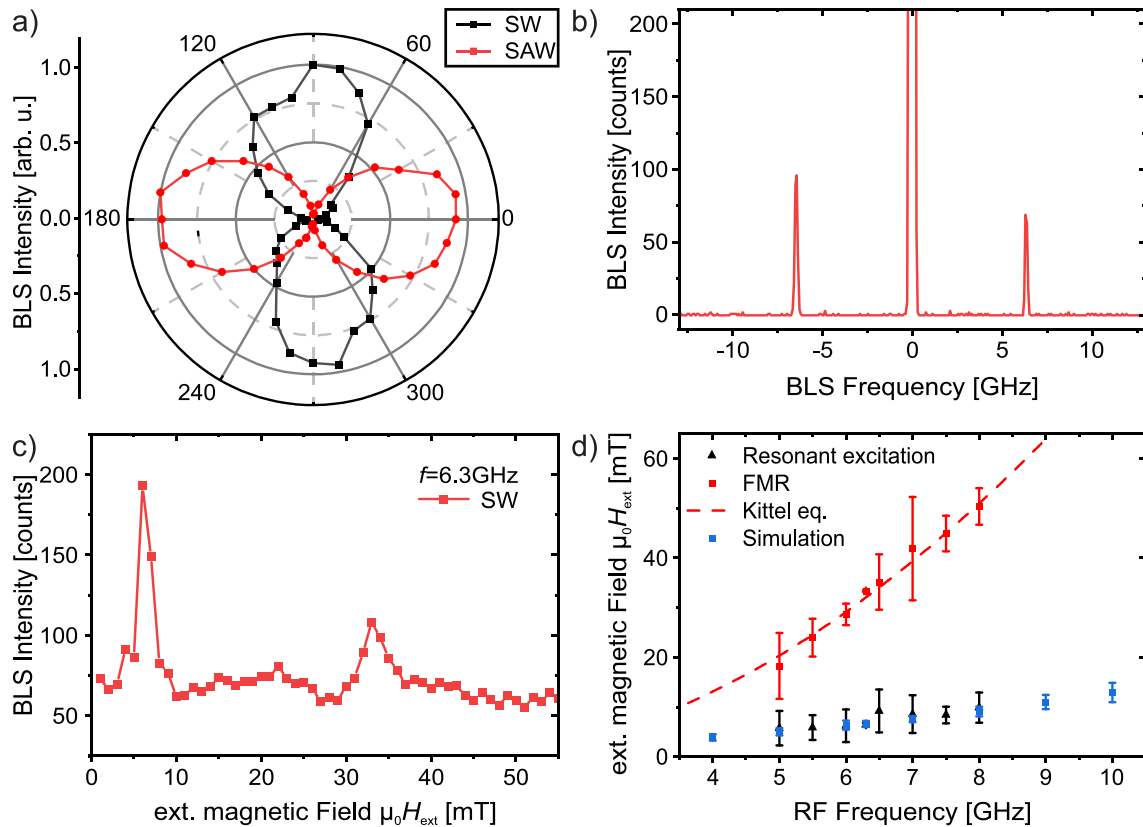


FIG. 2. (a) Normalized BLS intensity as a function of the polarization. The polarization of the light scattered by magnons is rotated by $\pi/2$, while the light scattered by the Rayleigh mode is unchanged in polarization. (b) BLS spectrum from spin waves excited by SAWs at a frequency of $f = 6.3$ GHz and an external field of $\mu_0 H_{\text{ext}} = 6$ mT. (c) BLS intensity as a function of the external magnetic field. Two peaks can be identified corresponding to the FMR (higher fields) and to a wave-vector preserving spin-wave excitation (lower fields). (d) Extracted field values from μ BLS measurements for FMR (red) and resonant excitation (black). FMR data are approximated using the Kittel equation [Eq. (1)]. The field values for the resonant excitation from micromagnetic simulations are shown in blue.

spin waves where both energy and linear momentum are conserved as will be discussed in detail further below.

Since the IDTs have a finite length, they have a finite bandwidth in which SAWs can be excited. In this case, the excited wave vector of the waves adapts to the dispersion of the excited frequency and the intensity of the SAWs decreases drastically.³² However, since the scattering process is a linear process, qualitatively similar results can be observed for frequencies not coinciding with the IDT resonance. Figure 2(d) shows the bias field values of the intensity maxima for different excitation frequencies. The maxima at higher field values (red) correspond to the FMR²³ and can be described very well by the Kittel formula:³⁵

$$f = \frac{\gamma \mu_0}{2\pi} \sqrt{(H_{\text{eff}} + H_k \cos(\varphi))(H_{\text{eff}} + H_k \cos(\varphi) + M_S)}. \quad (1)$$

A saturation magnetization of $M_S = 1150$ kA/m and a gyromagnetic ratio of $\gamma = 182$ rad/nsT are found. Furthermore, a small unidirectional anisotropy field $H_k = 2.91$ mT pointing along the x-axis is included (see the [supplementary material](#)). For the spin waves excited at low fields, only a slight increase in resonance field with the excitation frequency is visible. In the following, using micromagnetic

simulations, we will illustrate that this excitation is the result of a direct conversion of a phonon into a magnon, in which both the frequency and the wave vector is preserved. Since the wave vector of the SAW increases almost linearly with its frequency, the resonance field for the resonant scattering to the spin wave of the same frequency is increasing only slightly, in contrast to the excitation of the FMR.

To verify our hypothesis, we conduct micromagnetic simulations using Mumax3.³⁶ The software platform Aithericon was used to automatically start and analyze the simulation series and to manage the produced data.³⁷ The parameters used for the simulation are as follows: $M_S = 1150$ kA/m, $A_{\text{ex}} = 15$ pJ/m, $B_1 = B_2 = -8.8$ MJ/m³,^{38,39} and $\alpha = 4.3 \times 10^{-3}$. For the uniaxial in-plane anisotropy along the x-axis, an anisotropy constant of $K_u = 1600$ J/m³ was used (see the [supplementary material](#)). The dimensions of the simulated rectangle corresponds to the experimental ones. The simulated volume is divided into $2560 \times 512 \times 1$ cells. To mimic the SAWs, we assume a plane wave for the strain components S_{xx} and S_{xz} with wave vector k_{SAW} and frequency f . The ratio of S_{xx} and S_{xz} is unity and their phase is shifted by $\pi/2$, which results in the approximation of circular motion. Mumax3 calculates the effective magnetic field resulting from the SAW (see the [supplementary material](#)). The amplitude of the acoustic wave is chosen

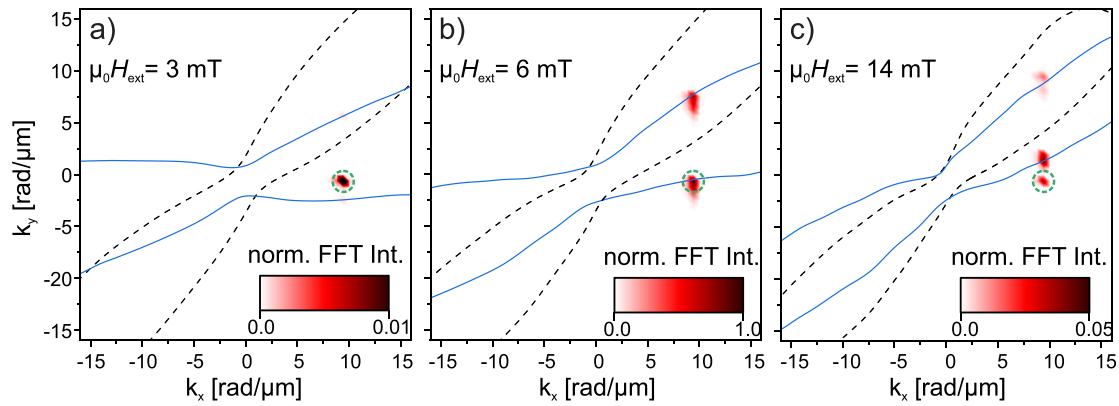


FIG. 3. Normalized spin-wave (FFT) intensity obtained from micromagnetic simulations in reciprocal space extracted for the SAW frequency $f_{\text{SAW}} = 6.3$ GHz for (a) $\mu_0 H_{\text{ext}} = 3$ mT, (b) $\mu_0 H_{\text{ext}} = 6$ mT, and (c) $\mu_0 H_{\text{ext}} = 14$ mT. The isofrequency curves for the investigated structure and an infinitely extended film were achieved by a point-like source and are shown in solid blue and dashed black lines, respectively. The excitation with the wave vector of the SAW, which is only resonant for $\mu_0 H_{\text{ext}} = 6$ mT, is indicated by green circles.

small enough such that non-linear effects in the spin-wave system can be neglected.

By performing a Fourier transform of the dynamic magnetization components in time and space, we obtain the spin wave intensity in k -space. To determine which wave vectors are excited, Fig. 3 shows in color-code the simulated spin-wave intensity in reciprocal space exemplary for the frequency $f_{\text{SAW}} = 6.3$ GHz. It can be seen that the magneto-elastic field generated by the SAWs drives the magnetization for all fields with the wave vector of the SAWs, which is indicated by green circles. However, this excitation is not necessarily an eigenstate of the magnonic system, and relaxation into states on the isofrequency curve (illustrated in blue) occurs. During the relaxation, the wave vector along the propagation direction of the SAWs (x -axis) is preserved. Most importantly, at $\mu_0 H_{\text{ext}} = 6$ mT, it can be seen that the direct excitation by the magneto-elastic field coincides with the magnonic isofrequency curve. This results in a resonant excitation that shows a drastically increased amplitude (note the different scales), in good agreement with the experimental findings in Fig. 2(c). To obtain a quantitative picture, we compare the excited spin-wave intensity in the simulations with our experimental results. Since μ -BLS collects all spin waves up to maximum wave vector $k_{\text{max}} = 16$ rad/ μm , the simulated spin-wave intensities are also integrated up to this value. The obtained values are shown in Fig. 4 for different external fields. All curves show a clear maximum at low magnetic fields, which corresponds to the resonant excitation. The extracted values are shown in blue in Fig. 2(d) and match well to the measured values of the resonant excitation. A closer analysis of the micromagnetic simulations shows that the intensity for fields above the FMR decreases drastically, since in this region only the excitation of edge modes is possible. However, there is no intensity peak associated with the FMR in the simulations. Further investigations on extended films have shown that the resonance attributed to the FMR cannot be observed there, which leads to the conclusion that the excitation might be attributed to a parasitic mechanism. We have identified two possible explanations for this occurrence of the FMR excitation in the experiments. The first and most likely mechanism that might lead to the excitation of the FMR is caused by the electromagnetic near-field of the IDT. The other possible

mechanism is due to scattering effects caused by inhomogeneities or the edge of the magnetic rectangle, which break the translation symmetry.

We would like to note that in the particular case of this study, the resonant excitation is possible due to the anisotropy present in the magnetic structures. This anisotropy is composed of the shape anisotropy of the micro-structure and the uniaxial in-plane anisotropy, which presumably originates from the film growth process. In an infinitely extended film without any anisotropies, the magnetization points always along the external magnetic field. In the present case, this implies that the magnetization always remains at 45° to the wave vector of the SAWs. For CoFeB rectangles of finite width, however, the anisotropy causes the magnetization not to point in the same direction as the external field at low magnetic fields, but to turn toward the direction of the long axis (x -direction). This is clearly shown by the isofrequency curves in Figs. 3(a)–3(c), which are extracted from micromagnetic

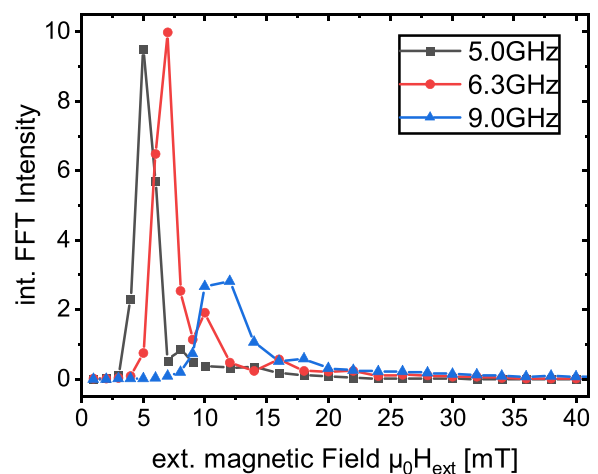


FIG. 4. Integrated spin-wave intensity from micromagnetic simulations for different SAW frequencies as a function of the external field. The peaks are associated with the fully resonant excitation of spin waves by the SAWs.

simulations using a spin-wave point source. The isofrequency curves for an infinitely extended film, which are shown by the dashed black lines, were simulated using periodic boundary conditions. These isofrequency curves are always rotated 45° to the wave vector of the SAWs. The isofrequency curves for finite structures, shown in blue, on the contrary, rotate with decreasing external field toward the propagation direction of the SAWs. In the present system this makes the overlap between the wave vector of the SAWs and that of the spin waves possible in the first place.

To conclude, in this work, we have studied the excitation of spin waves by surface acoustic waves in micrometer-sized CoFeB rectangles. Our investigations with micro-focused BLS spectroscopy have demonstrated that spin waves can be excited linearly with the frequency of the SAW at two different magnetic fields. One excitation is identified as the FMR. The second excitation appears at low external magnetic fields. Through micromagnetic simulations, we were able to show that in this process the frequency and the wave vector of the SAW are transferred to the excited spin wave. Thus, energy and linear momentum are conserved in this phonon–magnon scattering process. This is a promising step toward a voltage-controlled excitation of spin waves for low-power consuming magnon computing.

See the [supplementary material](#) for an analysis of the magnetic anisotropy and a description of the implementation of magneto-elastic interaction in the micromagnetic simulations.

The financial support by the EU Horizon 2020 research and innovation program within the CHIRON project (Contract No. 801055) and by the Deutsche Forschungsgemeinschaft (DFG, German Research Foundation)—TRR 173 “Spin+X”-268565370 (Project B01) is gratefully acknowledged. D.N. acknowledges financial support from the Research Foundation—Flanders (FWO) through Grant No. 15B9121N. The authors would like to acknowledge Cosmin Romanitan for performing the XRD analysis of the GaN/Si wafer and M. Weiler for valuable discussions.

AUTHOR DECLARATIONS

Conflict of Interest

The authors have no conflicts to disclose.

DATA AVAILABILITY

The data that support the findings of this study are available from the corresponding author upon reasonable request.

REFERENCES

- G. E. Moore, *Electronics* **38**, 114 (1965).
- A. A. Serga, A. V. Chumak, and B. Hillebrands, *J. Phys. D* **43**, 264002 (2010).
- A. Khitun, M. Bao, and K. L. Wang, *J. Phys. D* **43**, 264005 (2010).
- A. V. Chumak, V. I. Vasyuchka, A. A. Serga, and B. Hillebrands, *Nat. Phys.* **11**, 453 (2015).
- V. Kruglyak, O. Demokritov, and D. Grundler, *J. Phys. D* **43**, 260301 (2010).
- P. Pirro, V. Vasyuchka, A. A. Serga, and B. Hillebrands, *Nat. Rev. Mater.* **6**, 1114 (2021).
- A. Papp, W. Porod, and G. Csaba, *Nat. Commun.* **12**, 6422 (2021).
- A. V. Chumak, A. A. Serga, and B. Hillebrands, *Nat. Commun.* **5**, 4700 (2014).
- T. Brächer, O. Boule, G. Gaudin, and P. Pirro, *Phys. Rev. B* **95**, 064429 (2017).
- M. Grassi, M. Geilen, D. Louis, M. Mohseni, T. Brächer, M. Hehn, D. Stoeffler, M. Bailleul, P. Pirro, and Y. Henry, *Phys. Rev. Appl.* **14**, 024047 (2020).
- K. Szulc, P. Graczyk, M. Mruczkiewicz, G. Gubbiotti, and M. Krawczyk, *Phys. Rev. Appl.* **14**, 034063 (2020).
- S. Klingler, P. Pirro, T. Brächer, B. Leven, B. Hillebrands, and A. V. Chumak, *Appl. Phys. Lett.* **105**, 152410 (2014).
- T. Fischer, M. Kewenig, D. A. Bozhko, A. A. Serga, I. I. Syvorotka, F. Ciubotaru, C. Adelman, B. Hillebrands, and A. V. Chumak, *Appl. Phys. Lett.* **110**, 152401 (2017).
- G. Talmelli, T. Devolder, N. Träger, J. Förster, S. Wintz, M. Weigand, H. Stoll, M. Heyns, G. Schütz, I. P. Radu, J. Gräfe, F. Ciubotaru, and C. Adelman, *Sci. Adv.* **6**, eabb4042 (2020).
- A. V. Sadovnikov, E. N. Beginin, S. E. Sheshukova, D. V. Romanenko, Y. P. Sharaevskii, and S. A. Nikitov, *Appl. Phys. Lett.* **107**, 202405 (2015).
- Q. Wang, M. Kewenig, M. Schneider, R. Verba, F. Kohl, B. Heinz, M. Geilen, M. Mohseni, B. Lägler, F. Ciubotaru, C. Adelman, C. Dubs, S. D. Cotozana, O. V. Dobrovolskiy, T. Brächer, P. Pirro, and A. V. Chumak, *Nat. Electron.* **3**, 765–774 (2020).
- A. Mahmoud, F. Ciubotaru, F. Vanderveken, A. V. Chumak, S. Hamdioui, C. Adelman, and S. Cotozana, *J. Appl. Phys.* **128**, 161101 (2020).
- M. Fiebig, *J. Phys. D* **38**, R123 (2005).
- G. A. Smolenskii and I. E. Chupis, *Sov. Phys. Usp.* **25**, 475 (1982).
- L. A. Shelukhin, N. A. Pertsev, A. V. Scherbakov, D. L. Kazenwadel, D. A. Kirilenko, S. J. Hämäläinen, S. van Dijken, and A. M. Kalashnikova, *Phys. Rev. Appl.* **14**, 034061 (2020).
- A. Khitun and K. L. Wang, *J. Appl. Phys.* **110**, 034306 (2011).
- S. G. Alekseev, S. E. Dizhur, N. I. Polzikova, V. A. Luzanov, A. O. Raevskiy, A. P. Orlov, V. A. Kotov, and S. A. Nikitov, *Appl. Phys. Lett.* **117**, 072408 (2020).
- L. Dreher, M. Weiler, M. Pernpeintner, H. Huebl, R. Gross, M. S. Brandt, and S. T. Goennenwein, *Phys. Rev. B* **86**, 134415 (2012).
- M. Küß, M. Heigl, L. Flacke, A. Hefele, A. Hörner, M. Weiler, M. Albrecht, and A. Wixforth, *Phys. Rev. Appl.* **15**, 034046 (2021).
- R. Verba, I. Lisenkov, I. Krivorotov, V. Tiberkevich, and A. Slavin, *Phys. Rev. Appl.* **9**, 64014 (2018).
- M. Küß, M. Heigl, L. Flacke, A. Hörner, M. Weiler, M. Albrecht, and A. Wixforth, *Phys. Rev. Lett.* **125**, 217203 (2020).
- M. Xu, K. Yamamoto, J. Puebla, K. Baumgaertl, B. Rana, K. Miura, H. Takahashi, D. Grundler, S. Maekawa, and Y. Otani, *Sci. Adv.* **6**, eabb1724 (2020).
- N. K. Babu, A. Trzaskowska, P. Graczyk, G. Centała, S. Mieszczak, H. Glowinski, M. Zdunek, S. Mielcarek, and J. W. Klos, *Nano Lett.* **21**, 946 (2021).
- C. Zhao, Z. Zhang, Y. Li, W. Zhang, J. E. Pearson, R. Divan, Q. Liu, V. Novosad, J. Wang, and A. Hoffmann, *Phys. Rev. Appl.* **15**, 014052 (2021).
- M. Kraimia, P. Kuszewski, J. Y. Duquesne, A. Lemaître, F. Margailan, C. Gourdon, and L. Thevenard, *Phys. Rev. B* **101**, 144425 (2020).
- T. Sebastian, K. Schultheiss, B. Obry, B. Hillebrands, and H. Schultheiss, *Front. Phys.* **3**, 35 (2015).
- M. Geilen, F. Kohl, A. Nicoloiu, A. Müller, B. Hillebrands, and P. Pirro, *Appl. Phys. Lett.* **117**, 213501 (2020).
- F. Ciubotaru, T. Devolder, M. Manfrini, C. Adelman, and I. P. Radu, *Appl. Phys. Lett.* **109**, 012403 (2016).
- J. Y. Duquesne, P. Rovillain, C. Hepburn, M. Eddrief, P. Atkinson, A. Anane, R. Ranchal, and M. Marangolo, *Phys. Rev. Appl.* **12**, 024042 (2019).
- C. Herring and C. Kittel, *Phys. Rev.* **81**, 869 (1951).
- A. Vansteenkiste, J. Leliaert, M. Dvornik, M. Helsen, F. Garcia-Sanchez, and B. Van Waeyenberge, *AIP Adv.* **4**, 107133 (2014).
- See aithericon.com for further details on the HPC platform.
- F. Vanderveken, J. Mulkers, J. Leliaert, B. Van Waeyenberge, B. Sorée, O. Zografos, F. Ciubotaru, and C. Adelman, *Phys. Rev. B* **103**, 054439 (2021).
- M. Gueye, F. Zighem, M. Belmeguenai, M. S. Gabor, C. Tiusan, and D. Faurie, *J. Phys. D* **49**, 145003 (2016).